frontiers | Frontiers in Energy Research

TYPE Original Research
PUBLISHED 07 September 2022
DOI 10.3389/fenrg.2022.966852

OPEN ACCESS

EDITED BY
Jinliang Yuan,
Ningbo University, China

REVIEWED BY
Linfei Yin,
Guangxi University, China
Jingbo Wang,
Kunming University of Science and Technology, China

*CORRESPONDENCE
JianFeng Zhao,
jianfeng62300_zhao@163.com

SPECIALTY SECTION
This article was submitted to Fuel Cells, Electrolyzers and Membrane Reactors, a section of the journal Frontiers in Energy Research

RECEIVED 11 June 2022
ACCEPTED 04 August 2022
PUBLISHED 07 September 2022

CITATION
Liang Y, Liang Q, Zhao J and He J (2022), Minimum hydrogen consumption power allocation strategy for the multi-stack fuel cell (MFC) system based on a discrete approach.
Front. Energy Res. 10:966852.
doi: 10.3389/fenrg.2022.966852

Minimum hydrogen consumption power allocation strategy for the multi-stack fuel cell (MFC) system based on a discrete approach

YiFan Liang, QianChao Liang, JianFeng Zhao* and JunNeng He

Naval University of Engineering, Wuhan, China

In high-powered application scenarios, a multi-stack fuel cell system (MFCS) could have advantages such as higher robustness, lifetime, and reliability than a single-stack fuel cell system. In particular, MFCS could maintain a high efficiency and increase system redundancy by power configuration between subsystems. In order to reduce the operational expenses for systems, a reasonable power management strategy is necessary to minimize the hydrogen consumption of MFCS. First, the power-hydrogen consumption curve of the single-stack fuel cell system is discretized from experimental measurements. Next, the discrete data are reassembled by the inverse derivation of the dynamic programming method to produce a minimum solution for the hydrogen consumption in the output power range. It is found that the strategy varies depending on activated state On or Off. Finally, two power allocation strategies are developed and modeled in a lookup-table block considering the activated state. The optimal stack output power strategy is analyzed with four stacks. The results indicate that the hydrogen consumption is smaller and more efficient than the other allocation strategies. It can respond to the load demand with a high efficiency sooner than the average strategy.

KEYWORDS

MFC system, dynamic programming, discrete, minimum hydrogen consumption, power allocation

1 Introduction

Hydrogen fuel cell systems are an attractive long-term option for the environment because of their zero-emission and high efficiency. As the electricity demand has increased, fuel cells have gradually tended to be high-powered and large-sized. However, this also means that fuel cells require higher power compressors and other auxiliary facilities, leading to higher fuel cell costs. Moreover, with the current technology development, it is challenging to realize high-power single-stack fuel cells for large load

structures such as trams and microgrids. With this background, multi-stack fuel cell structures are gradually coming into view (Marx et al., 2014).

The optimal efficiency range of single stack fuel cells is 40–45%, but it is difficult to maintain due to load power fluctuation. To keep the system in the high-efficiency region, increasing the number of fuel cell systems and fitting with a power allocation strategy improve Proton exchange membrane fuel cell (PEMFC) degree of freedom (Garcia et al., 2014). Under the same working condition and fuel utilization rate, the PEMFC system with a multi-stack structure can improve fuel utilization and the system efficiency (Pirasaci, 2019).

After research, the parallel structure is more suitable for multi-stack fuel cell systems. Benefiting from the parallel structure, a degradation operation can exclude the faulty stack from the multi-fuel cell system (MFC system). The stack is replaced when a stack fails (Becherif et al., 2015). The multi-stack association appears as a natural and necessary alternative for developing high-power fuel cell systems. Bernardinis (De Bernardinis et al., 2008) proposed a solution for the parallel structure of two (or more) fuel cell stacks: parallel and series electrical coupling through power converters for fuel cell systems. Numerical simulations of the assembled dual-stack PEMFC demonstrate exemplary performance. Both research and experimental validation prove the technical feasibility of the dual-stack PEMFC parallel architecture.

The power allocation for the MFC system focuses on performance consistency, efficiency, hydrogen consumption, and costs. In particular, the cost will focus on determining the efficiency of MSFC solutions. The industry will welcome MFC systems if the expenses are solved (Marx et al., 2014).

Wang (Wang et al., 2020) believe that the degradation rate of poor-performance stacks is faster and affects the performance of MFCS systems. The degree of performance degradation (DOPD) adopts a semi-empirical model to evaluate the effect of aging on stacks. Subsequently, an adaptive current distribution method is proposed considering FC performance consistency implemented with instantaneous virtual resistance calculation and the virtual sag technique of R_{droop} (Wang et al., 2019a). The experimental results show that the method can protect the poor performance stack, improve the MFC system life, and have better current control and load voltage regulation capabilities. Meng (Meng et al., 2020) proposed a distributed control strategy to keep the same degradation for FCs in MFCS, which considered multi-stack fuel cells and energy storage elements as a multi-agent system (MAS). It was applied to structures of the MFC system and concluded that parallel is the best.

Zhang (Zhang et al., 2021) proposed an improved overall efficiency maximization strategy (I-OEMS), which predicts the load variation and controls the output power of the subsystem in a gentle loading manner, ensures that the system efficiency is close to optimal and reduces hydrogen consumption, and improves loading conditions to protect the stack. Francisco (Lopes et al., 2016) used NARX and NOE neural network modeling to predict stack performance. The controller is designed with efficiency maximization for the power allocation strategy. The model still performs better against lower currents with nonlinear ranges and peaks. Marx (Marx et al., 2018) analyzed the nonlinear programming by the KKT (Karush–Kuhn–Tucker) approach, which obtained an analytic solution to MFC system efficiency. Also, it provides a simple and effective solution to power allocation. Compared with average and daisy-chain strategies, better results than the existing strategies are obtained. Zhou (Zhou et al., 2022a) investigates a two-stack optimization problem with an efficiency and remaining useful life (RUL) factor-based power allocation. A heavy vehicle with a full load of 40t has experimented with the results of optimal configuration with three to five stacks. Compared with single FCS, MFCS has more efficiency and longer RUL as the number of MFCS stacks increases. Fernandez (Fernandez et al., 2019) updated the real-time ME (maximum efficiency) and MP (maximum power) of each sub-stack through a multi-physics model integrated with a semi-empirical model using as few sub-stacks as possible to satisfy loading power. Three scenarios measure the method, and it was found to be more efficient and less hydrogen-consuming than the average and daisy-chain strategy. Han (Han et al., 2017) separated the MFC system into main and sub-stacks, controlling the auxiliary stack On and Off by determining the threshold value after an efficiency optimization allocation strategy. The proposed efficiency and transient optimization strategies can significantly reduce fuel consumption and keep the output power of both stacks in the high-efficiency operating region. Bouisalmane (Bouisalmane et al., 2021) developed a power allocation strategy utilizing a particle swarm intelligence algorithm (PSO). Experiments were conducted with two output powers in 25–280W and 25–320W, and the results showed that the proposed method has the best performance in reducing hydrogen consumption. Macias (Macias et al., 2018) used a semi-empirical model combined with the ARLS algorithm, introduced adaptive parameters to realize online control of the MFC system, and solved online the maximum power and optimal efficiency of each fuel cell. The required power, MP, and ME points of each PEMFC are used as input to determine the output power of each PEMFC. Wang (Wang et al., 2019b) utilizes forgetting factor recursive least squares (FFRLS) to control minimum hydrogen consumption in a dual-stack system online. Reducing the effect of initial data on recursion by adding forgetting factors is validated by building a two-stack fuel cell system.

Calderon (Calderón et al., 2020) proposes a generalized state space model for MFC systems, where the power allocation is based on the degree of stack degradation, combined with an MPC controller for reducing the system degradation. Jian (Jian and Wang, 2022) presents a fuel cell electric vehicle (FCEV) power system model to MFC systems to increase system redundancy. A

TABLE 1 Parameters for model calibration.

	FC1	FC2	FC3	FC4
ξ_1	0.979511192288	0.972380580235	0.971943642250	0.972010958400
ξ_2	−0.0167801035044	−0.0226199947788	−0.0229778420499	−0.0229227111340
ξ_3	0.137687203210064	0.185605757126	0.188542031752	0.188089660715
ξ_4	0.00340652205626	0.000152650017836	0.000166275814243	0.00018186889999
ζ_1	3.62154231456e-08	5.85024983613e-08	2.64536727339e-08	−7.34325522541e-09
ζ_2	2.99598886498e-05	−1.76920183998e-05	5.74636139701e-05	0.000124656557481
ζ_3	−1.10486182104e-05	−1.78939545395e-05	−7.89798289321e-06	2.00685738939e-06
B	1.00679262149767	0.00917112012674	0.00931617010918	0.00929376566213

rule-based energy management strategy (REMS) is proposed to enable the MFC system to operate in an efficient region. Li (Li et al., 2021) proposed that an increment-oriented power distribution strategy to achieve the online collaborative performance enhancement between fuel economy and durability for the parallel multi-stack architecture. Andujar's (Andújar et al., 2022) MFCS-based solution built with an air-cooled multi-stack fuel cell (ACFC) provides greater flexibility, robustness, and resilience to hydrogen systems at a lower cost and also allows the power to be adjusted to the power required by the microgrid. Zhou (Zhou et al., 2022b) made a decision model of MFCS stack allocation, and the related power management for the application of heavy-duty commercial vehicles is established with an integrated optimization index of efficiency and RUL and co-solved by iterative and heuristic algorithms.

In summary, most of the existing algorithms have the following disadvantages: 1) strategies based on metaheuristic algorithms may fall into local optimal, 2) most power allocation strategies have not considered the differences in power stack characteristics within a multi-stack system, and 3) most power allocation strategies were comparable with average and Daisy chain, but without comparison between optimization strategies. In this article, we aim to find the optimal solution under minimum hydrogen consumption conditions.

Many scholars have adopted the DP algorithm to solve the discrete problem of energy management (Cardozo, 2015; Cheng et al., 2015; Zhang and Xiong, 2015; Liu et al., 2017), which finds the optimal one after comparing all possible suboptimal solutions by traversal. In this study, the single-stack fuel cell power-hydrogen consumption curve is discretized. The final model is a lookup table of power-single stack power, computed by the DP algorithm to find the power strategy for the minimum hydrogen consumption. The resulting power allocation strategy is expressed as starting with a few power stacks to satisfy the power demand, consistent with (Marx et al., 2017). This strategy avoids excessive auxiliary losses and delays the stacks' degradation. MFCS allocation is through online interpolation and search.

2 Multi-stack fuel cell system model

In this article, the MFC system was designed based on the T-1000 PEMFC system from Troowin company, which has a cooling system and anode oxygen consisting of an airflow generated by a fan to the side of the stack. The FC-related parameters are shown in Table 1.

Figure 1 shows four stacks' experimental values. FCs have different peak powers due to different degradations, as shown in Figure 1A. The hydrogen consumption curve of each stack is fundamental to search for the optimal power combination under minimum hydrogen consumption, as shown in Figure 1B.

The MFC system's conception is parallel. Fuel cells connect to the bus through a DC/DC converter, which then connects to the load. The MFC system power allocation strategy regulates the output power of each subsystem through the DC/DC converter.

2.1 PEMFC system model

Under the normal operating conditions, the output voltage of the fuel cell is less than the theoretical Nernst voltage E_{nerst} due to fuel cell activation loss, Ohmic loss, and concentration losses [15]. The charge double layer effect is added using the proposed structure in Musio et al., 2011a. The general equation for calculating the FCS output voltage (V_{FCS}) is as follows:

$$V_{FCS} = N\left(E_{\mathrm{Nernst}} + V_{\mathrm{act}} + V_{\mathrm{ohmic}} + V_{\mathrm{con}}\right) \tag{1}$$

where N is the number of cells, E_{Nernst} is the reversible cell potential (V), V_{act} is the activation loss (V), V_{ohmic} is the Ohmic loss (V), and V_{con} is the concentration loss. The E_{Nernst} is determined by

$$E_{\mathrm{Nernst}} = 1.229 - 0.85 \times 10^{-3}\left(T_{st} - 298.15\right) + 4.3085 \times 10^{-5} T_{\mathrm{st}}\left[\ln\left(P_{H2}\right) + 0.5\ln\left(P_{O2}\right)\right] \tag{2}$$

where T_{st} is the stack temperature (K), $P_{\mathrm{H_2}}$ is the hydrogen partial pressure in the anode side (Nm^{-2}), and P_{O_2} is the oxygen partial pressure on the cathode side (Nm^{-2}).

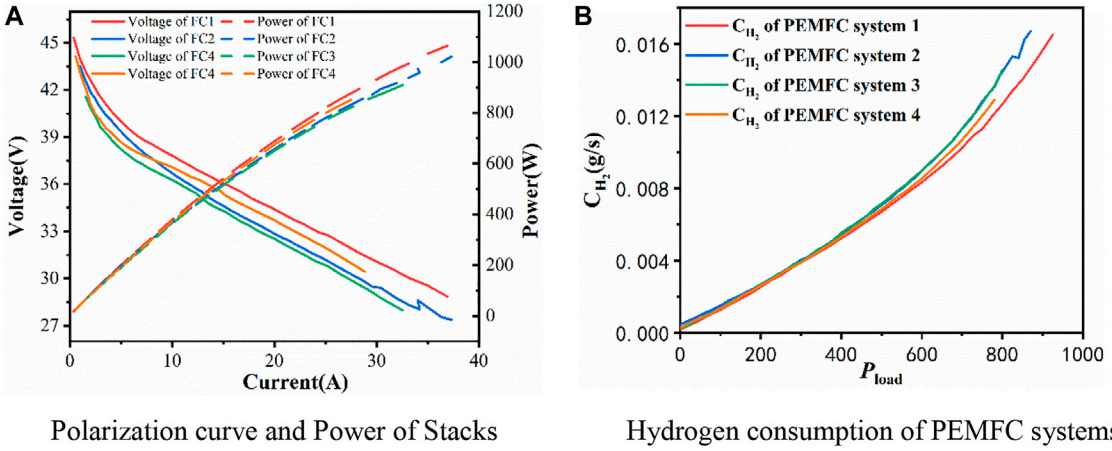

FIGURE 1
PEMFC characteristic curve on experiment data. **(A)** Polarization curve and power of stacks. **(B)** Hydrogen consumption of PEMFC systems.

2.2 Polarization loss

2.2.1 Activation loss

Activation loss indicates the slowness of the electrochemical reactions on the electrode surface, which is the function of temperature and current. Also, it is divided into temperature-dependent activation loss (Vacc1) and current and temperature-dependent activation loss (Vacc2) based on (Cheng et al., 2015).

$$V_{act} = -[\xi_1 + \xi_2 T_{st} + \xi_3 T_{st} \ln(\mathrm{CO}_2) + \xi_4 T_{st} \ln(i_{FCS})] \quad (3)$$

$$V_{act1} = -[\xi_1 + \xi_2 T_{st} + \xi_3 T_{st} \ln(\mathrm{CO}_2)] \quad (4)$$

$$V_{act2} = -[\xi_4 T_{st} \ln(i_{FCS})] \quad (5)$$

$$C_{O_2} = P_{O2}/5.08 \times 10^6 \exp(-498/T_{st}) \quad (6)$$

where $\xi_n\,(\mathrm{n} = 1 \ldots 4)$ are empirical parameters, CO_2 is the oxygen concentration (mol cm^{-3}), and i_{fcs} is the FC current (A). The equivalent resistance of activation (R_{act}) corresponding to V_{act2} is obtained by V_{act2}/i_{FCS}.

2.2.2 Ohmic loss

Ohmic loss includes the resistance of the film resistance, the conductive resistance between the film and electrode, and the electrode resistance (Kristianda, 2018). The Ohmic loss is expressed by

$$V_{\mathrm{ohmic}} = -i_{FCS} R_{\mathrm{intern}} = -i_{FCS}(\zeta_1 + \zeta_2 T_{st} + \zeta_3 i_{FCS}) \quad (7)$$

where R_{intern} is the internal resistance (Ω) and $\zeta_n\,(\mathrm{n} = 1 \ldots 3)$ are empirical parameters.

2.2.3 Concentration loss

Concentration loss V_{conc} is the result of the reactant diffusion hysteresis phenomenon caused by

The differential concentration among main gas and reactant concentrations on the electrode catalytic active surface (Musio et al., 2011b; Kristianda, 2018), expressed by

$$V_{\mathrm{con}} = B \ln\left(1 - \frac{J}{J_{max}}\right) \quad (8)$$

where B is empirical, J indicates the current density (A cm^{-2}), and J_{max} is the maximum current density (A cm^{-2}). The equivalent resistance of concentration (R_{con}) is obtained by V_{con}/i_{FC}. The charge double layer phenomenon, which is formed along with the porous cathode and the membrane when sudden significant changes happen in a short time, is obtained by (Salim et al., 2015)

$$V_C = (i_{FCS} - cdV_C/dt)(R_{act} + R_{con}) \quad (9)$$

where V_C is the double layer charging effect (V) and V is the capacitance (F), which can be in the order of several farads since the PEMFC electrodes are porous. By taking the double layer effect into account, the output voltage of the FCS needs to be reformulated as

$$V_{FCS} = N(E_{\mathrm{Nernst}} + V_{\mathrm{act1}} + V_C + V_{\mathrm{ohmic}}) \quad (10)$$

2.3 DC/DC convert

The fuel cell output characteristic is soft, which shows that the voltage decreases gradually when the output power increases. A DC/DC convert is adopted to fix the voltage. The fuel cell output power indirectly controls the output voltage and current of the DC/DC converter. The control

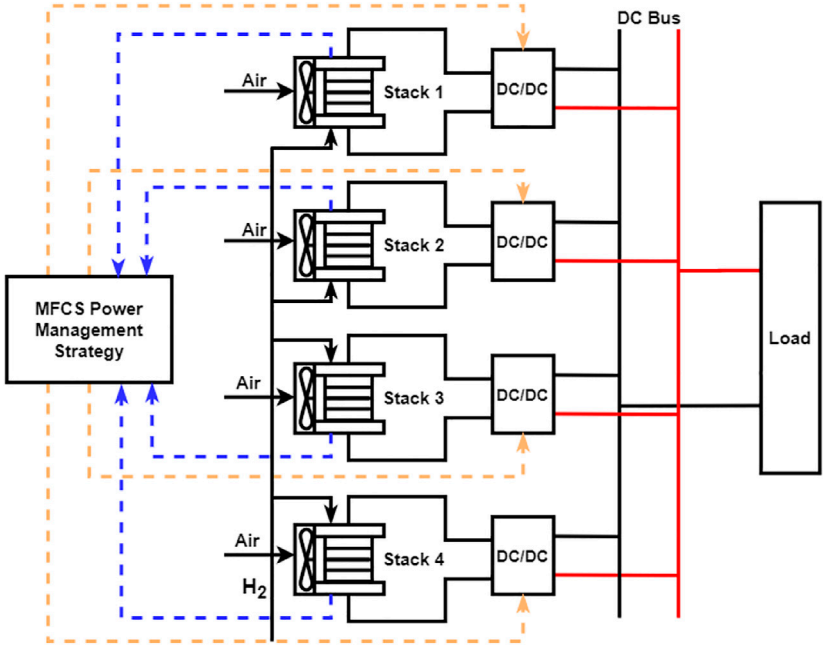

FIGURE 2
MSFCS architecture.

strategy is based on De Bernardinis et al., 2008; Becherif et al., 2015; Abuzant et al., 2017.

This study uses DC/DC converters in parallel architecture as power converters, as shown in Figure 2. This architecture makes the overall system more flexible and enables individual control of each fuel cell stack for energy management. In power calculations, the boost DC/DC converter is treated as a constant efficiency expression, as follows:

$$P_{load} = \eta_{DC/DC} P_{fcs} \tag{11}$$

where P_{load} is the load power, $\eta_{DC/DC}$ is the efficiency of the DC/DC converter, which is regarded as a constant of 0.98, and P_{fcs} is the output power of the PEMFC system.

3 MFC system characterization

3.1 Single-stack system characterization

The efficiency of the PEMFC stack is given by Eq. 12:

$$\eta_{FC} = \frac{P_{SFC}}{P_{H2}} \times 100\% = \frac{V_{SFC} \times n \times F}{\Delta H} \times 100\% = \frac{V_{SFC}}{1.482} \times 100\% \tag{12}$$

η_{FC} is the efficiency of the stack, P_{SFC} is the stack power, P_{H2} is total hydrogen energy consumed, I_{FC} is the stack output current, V_{SFC} is the cell voltage, F is the Faraday constant, ΔH is the heat value of hydrogen, and n is the number of atoms involved in chemical reactions. (Please note nF / ΔH = 1.482V when ΔH = 286 kJ/mol). Since the FC's voltage decreased as the stack power increased, DC/DC converts match fuel cells as an essential electrical component. PEMFC system efficiency inevitably contains the DC/DC convert energy loss. A PEMC system consists of a stack, controller, and dc/dc convert. Eq. 11 is modified based on the system structure as Eq. 13:

$$\eta_{FCS} = \frac{V_{SFC}}{1.254} \times \frac{P_{FC} - P_{aux}}{P_{FC}} \times 100\% = \eta_{FC} \times \eta_{aux} \times \eta_{ele} \tag{13}$$

η_{FCS} is the PEMFC system efficiency, P_{aux} is the accessory power, η_{FC} is the stack efficiency, η_{aux} is the accessory efficiency, and η_{ele} is the DC/DC convert efficiency, set to 95% for calculations. nF / ΔH = 1.254V due to air-cooled FC.

$$C_{H_2} = \Delta H \frac{I}{nF} \tag{14}$$

C_{H_2} is the total amount of hydrogen energy consumed (J/s, W), ΔH is the high heating value of hydrogen, I is the current, n is the number of atoms involved in the reaction, and F is the Faraday constant.

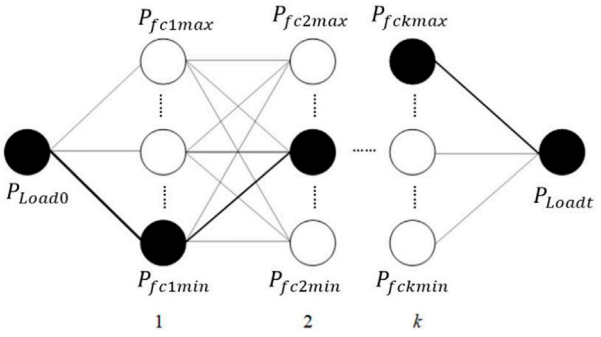

FIGURE 3
Dynamic programming algorithm.

3.2 MFC system hydrogen consumption and efficiency

Eq. 14 extends to a multi-stack with the following expression:

$$C_{MFCS} = \frac{\Delta H\left(I_1 + I_2 + \ldots + I_n\right)}{nF} \tag{15}$$

The efficiency of the dual-stack fuel cell system is shown in Eq. 15

$$\eta_{MFCS} = \frac{nFP_{MFCS}}{\Delta H\left(I_1 + I_2 + \ldots + I_n\right)} = \frac{P_{MFCS}}{\frac{P_{FCS1}}{\eta_{FCS1}} + \frac{P_{FCS2}}{\eta_{FCS2}} + \ldots + \frac{P_{FCSn}}{\eta_{FCSn}}} \tag{16}$$

P_{MFCS} indicates the total power of the dual-stack fuel cell, whose value is $P_{FCS1} + P_{FCS2} + \ldots + P_{FCSn}$; P_{FCSn} and η_{FCSn} indicate the distributed power and the system efficiency of fuel cell system n, respectively.

4 Discrete optimal strategy

After discretizing all fuel cell subsystems of load-hydrogen consumption, the DP algorithm is applied to get the power allocation matrix under the same load conditions, consisting of each subsystem's power and the hydrogen consumption. The DP algorithm avoids being trapped in the optimal local solution and is combined with the lookup table in Simulink to implement online interpolation for strategies. For the MFC system power allocation strategy, the hydrogen consumption of the MFC system, which is taken as a state variable, the hydrogen consumption–power curve is divided into steps of 0.5W, as shown in Figure 3.

The subproblem after splitting cannot form a square array similar to Yan et al., 2020 due to different degradation degrees in fuel cells. The constraints for the power and hydrogen consumption shown below should be satisfied.

TABLE 2 State machine control strategy.

P_{demand}	State	FC1	FC2	FC3	FC4
$P_{demand} \le P_{inter,1}$	1	On	Off	Off	Off
$P_{inter,1} \le P_{demand} \le P_{inter,2}$	2	On	On	Off	Off
$P_{inter,2} \le P_{demand} \le P_{inter,3}$	3	On	On	On	Off
$P_{inter,3} \le P_{demand}$	4	On	On	On	On

$$\operatorname{argmin}\left(C_{fcs1} + C_{fcs2} + \ldots + C_{fcsk}\right) \tag{17}$$

$$P_{load} = P_{fc1} + P_{fc2} + \cdots + P_{fck}k = 1, 2 \ldots, n \tag{18}$$

$$P_{fckmin} \le P_{fck} \le P_{fckmax} \tag{19}$$

where $C_{fcsk}\,(k = 1 \ldots n)$ is the hydrogen consumption of No. k, P_{load} is the total load power, P_{fck} is the output power of No. k, and P_{fckmin} and P_{fckmax} are the subsystem output power lower and upper border of No. k, respectively.

Subsystems have two states: On and Off. The state On represents that the stack is activated, and the hydrogen consumption at power output and the auxiliary consumption is also considered, especially at $P_{fck} = 0$. Although consumption is minor, it still affects the power allocation strategy under low power; the state Off denotes that the fuel cell is not activated and without consumption, as shown in Table 2.

There exist critical points $P_{inter,n}$, which indicate that MFCS and its degraded system have the same hydrogen consumption. A degraded system represents an MFC system with fewer activated stacks. When the MFC system's power is equal to $P_{inter,n}$, fewer stacks are activated to delay FC degradation as much as possible. This phenomenon is most pronounced when the subsystem state is Off, and the value of $P_{inter,n}$ will change as the subsystem is activated.

Finally, the power allocation strategy is shown in Figure 4. The MFC system consists of four fuel cells with 1 kW rated power. However, the maximum power presented is not the same due to individual stacks' degradation. The load power starts at 0W in steps of 10W and gradually increases to the peak (3470W).

Figure 4A shows that for all subsystems, the activated state is Off. The power allocation strategy reallocates power with the start of the subsystem at 10W, 860W, 230W, and 530W, as shown in Figure 4B. Although the peak power of FC2 is higher than that of FC3 and FC4, characteristics are better for FC3 and FC4 in the low output range than for FC2. The activation loss transforms to concentration loss, and the output power of FC2 gradually exceeds that of FC3 and FC4, with the load increasing. Figure 4C shows that all subsystems start in the standby state after one start-up. Contrary to other essays, the MFC power distribution curve is not smooth by DP programming. It is attributed to the inverse derivation process of dynamic

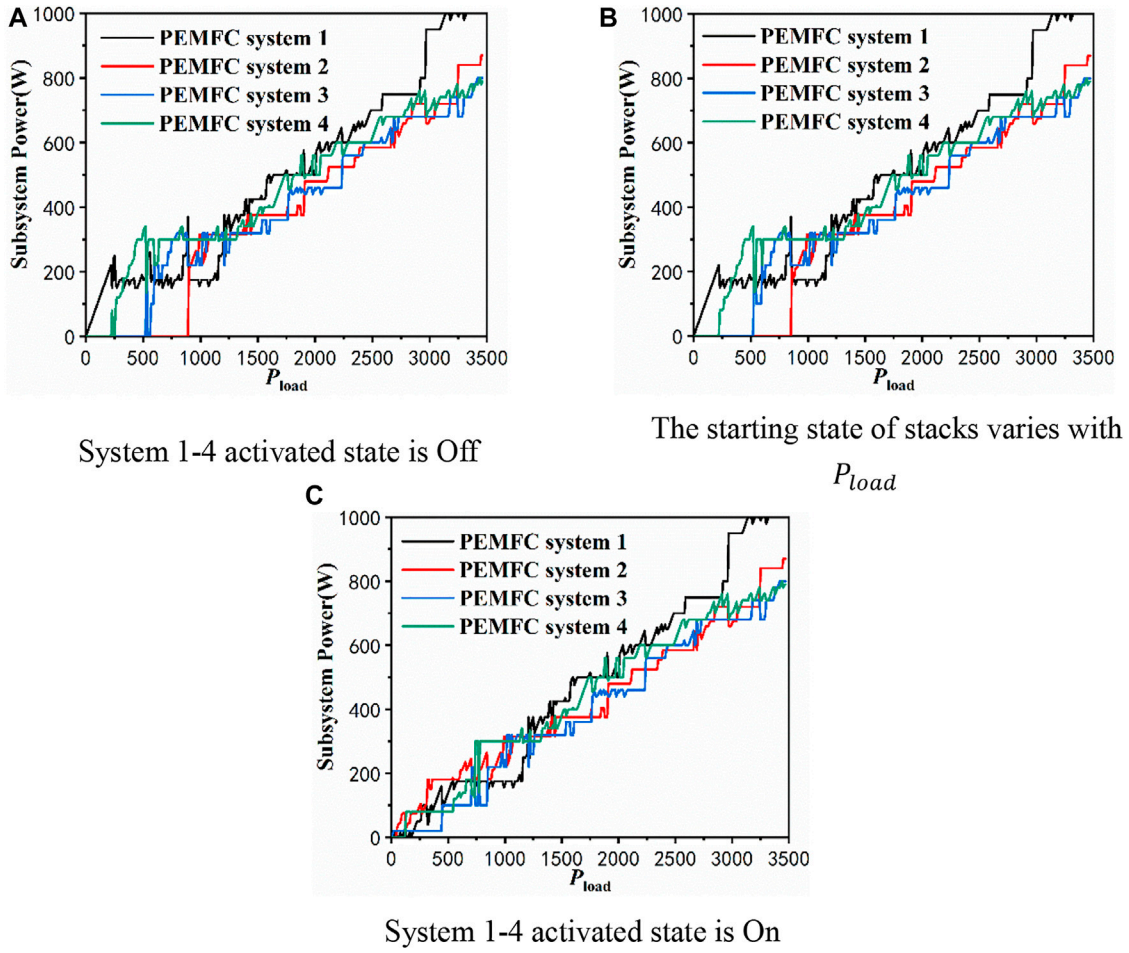

FIGURE 4
MFCS power allocation strategy. **(A)** Activated state of systems 1–4 is Off. **(B)** Starting state of stacks varies with P_{load}. **(C)** Activated state of systems 1–4 is On.

programming considering hydrogen consumption combinations for the optimal value.

5 The fault state

This approach also allows searching for the optimal power allocation solution when the power stack is faulty, enumerating all the situations with fault and reperforming power allocation of the MFC system with degradation. Stack No.4 is assumed to fail, as shown in Figure 5.

Figure 5 represents the degradation strategy with FC No.4 faults. The peak power decreases from 3470w to 2670w. The parameters of output power and hydrogen consumption are set to 0 for stack 4. Finally, the solution procedure in Section 4 is repeated for the three stack optimal power allocation strategies.

6 Simulation result and discussion

In this section, the proposed strategy is compared with the average and Daisy-chain strategies for hydrogen consumption and system efficiency and applied to the two load cycles for the three strategies to investigate the effect of activated state on power management. Finally, a shift in strategies for the MFC system occurs when one of the power stacks fails.

6.1 Power allocation strategy introduction

6.1.1 Average strategy

The distribution strategy is characterized by the same output power from subsystem fuel cells. It is expressed explicitly as

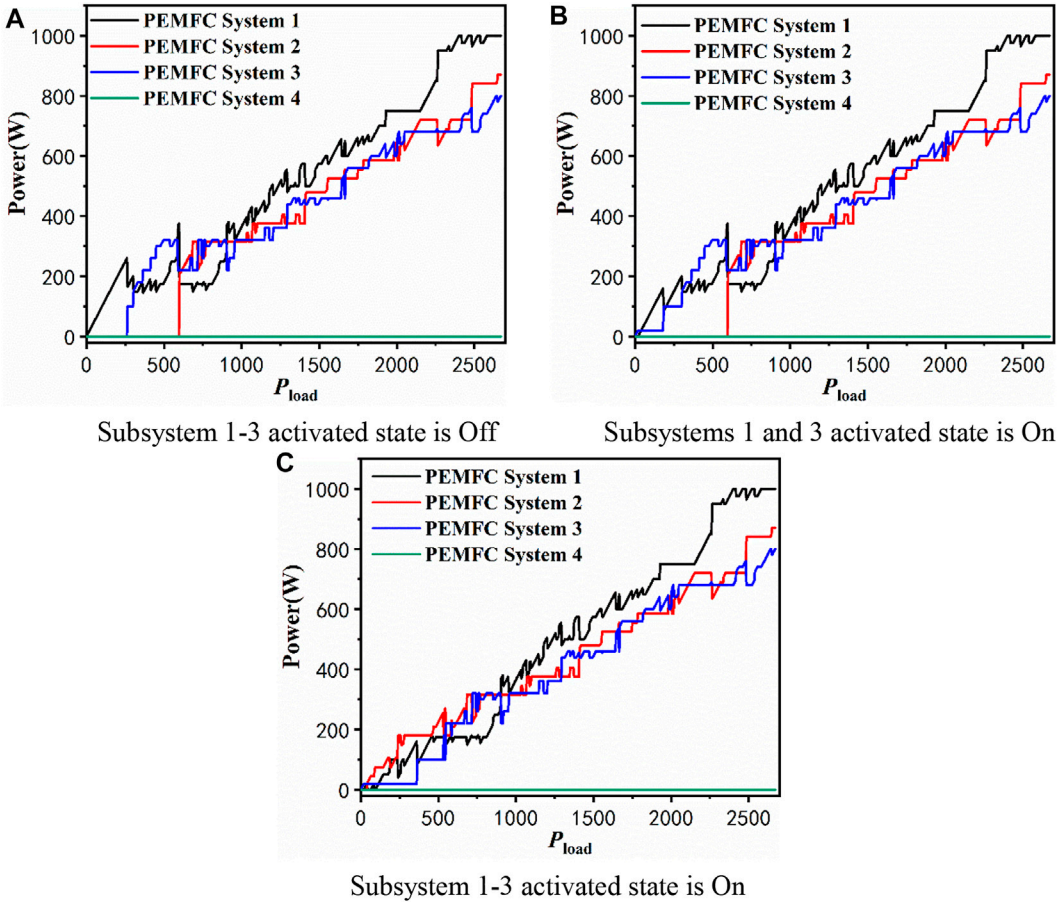

FIGURE 5
Power allocation strategy with FC4 fault. **(A)** Activated state of subsystems 1–3 is Off. **(B)** Activated state of subsystems 1 and 3 is On. **(C)** Activated state of subsystems 1–3 is On.

$$P_1 = P_2 = P_3 = \ldots = P_k = \frac{P_{load}}{k} \tag{20}$$

where k is the count of the FC subsystem and P_{load} is the total load power.

6.1.2 Daisy chain

The distribution strategy is characterized when the maximum output power is reached in the first fuel cell subsystem, and the following stack will be activated until the entire system meets the output requirement.

6.1.3 Performance of different strategies

The MFC system has the lowest hydrogen consumption compared to the other two algorithms (average and Daisy chain) as shown in Figure 6A. Interestingly, the strategy mentioned in this study will achieve the maximum efficiency point earlier than the average and has the same maximum efficiency as the Daisy chain. It is not necessary to activate all stacks when degraded MFCS can satisfy the load power and reduce the additional loss of electronic auxiliaries the same as the Daisy chain. Second, this feature can facilitate the development of hybrid energy power allocation.

6.2 Power distribution comparison

In this section, the load is running for 1,020 s in 10-s steps. The load is cycled twice to verify the effect of activated state for power allocation, as shown in Figure 7. P_{load} starts from 0 and gradually increases to the peak demand (2500W) with two cycles. The strategy proposed in this study is compared with the classical allocation strategies: average and Daisy chain applied too frequently varying loads for hydrogen consumption and system efficiency.

Four sub-systems have the same power values everywhere in average strategy, as shown in Figure 8A. Notably, the average distribution strategy determines the peak power of the worst-performing stack. Therefore, the MFC system must change the

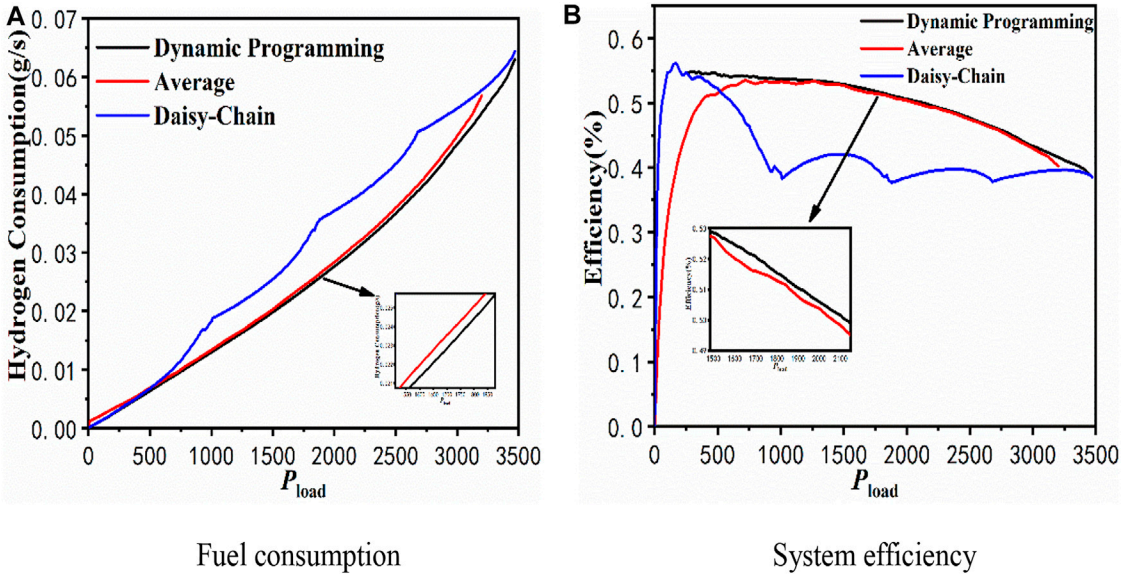

FIGURE 6
Comparision of different strategies. **(A)** Fuel consumption. **(B)** System efficiency.

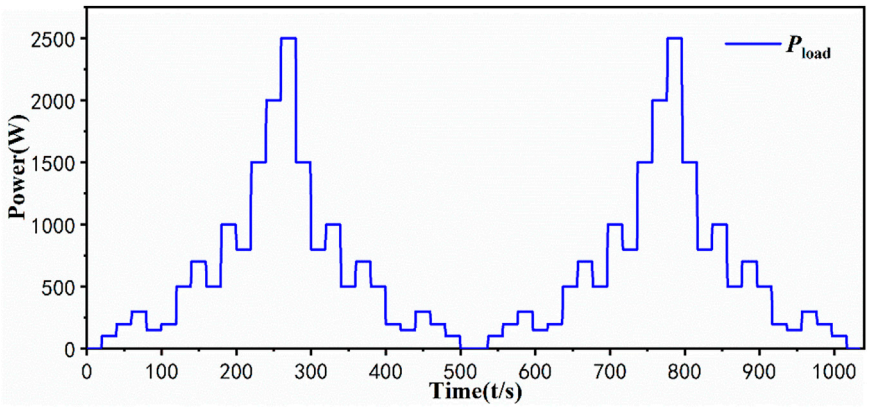

FIGURE 7
Demand power of the whole FCS.

maximum power from 3470 to 3200W in this paper. The power lost is not tolerated in the actual system. In the Daisy-chain strategy, the No.4 stack is static. The peak power of 2500W is less than the activation power of the fourth stack. However, FC1 and FC2 have reached their maximum capacity during this load response, as shown in Figure 8B.

The power allocation results for stages 1 and 2 are different, as shown in Figure 8C. Stacks 1–4 are activated at 22s, 181s, 60s, and 141s when the subsystem transforms to state On, followed by results in Section 3. During the transition from stage 1 to stage 2, the MFC system fuel consumption is not 0 when P_{load} = 0W, indicating that all subsystems are on at the initial state, and there is auxiliary power consumption, although the system does not perform external output.

A comparison of hydrogen consumption versus efficiency for the three strategies in the MFC system is shown in Figure 9. Interestingly, the Daisy-chain strategy has the fewest activated stacks, but its system hydrogen consumption is the most. Power

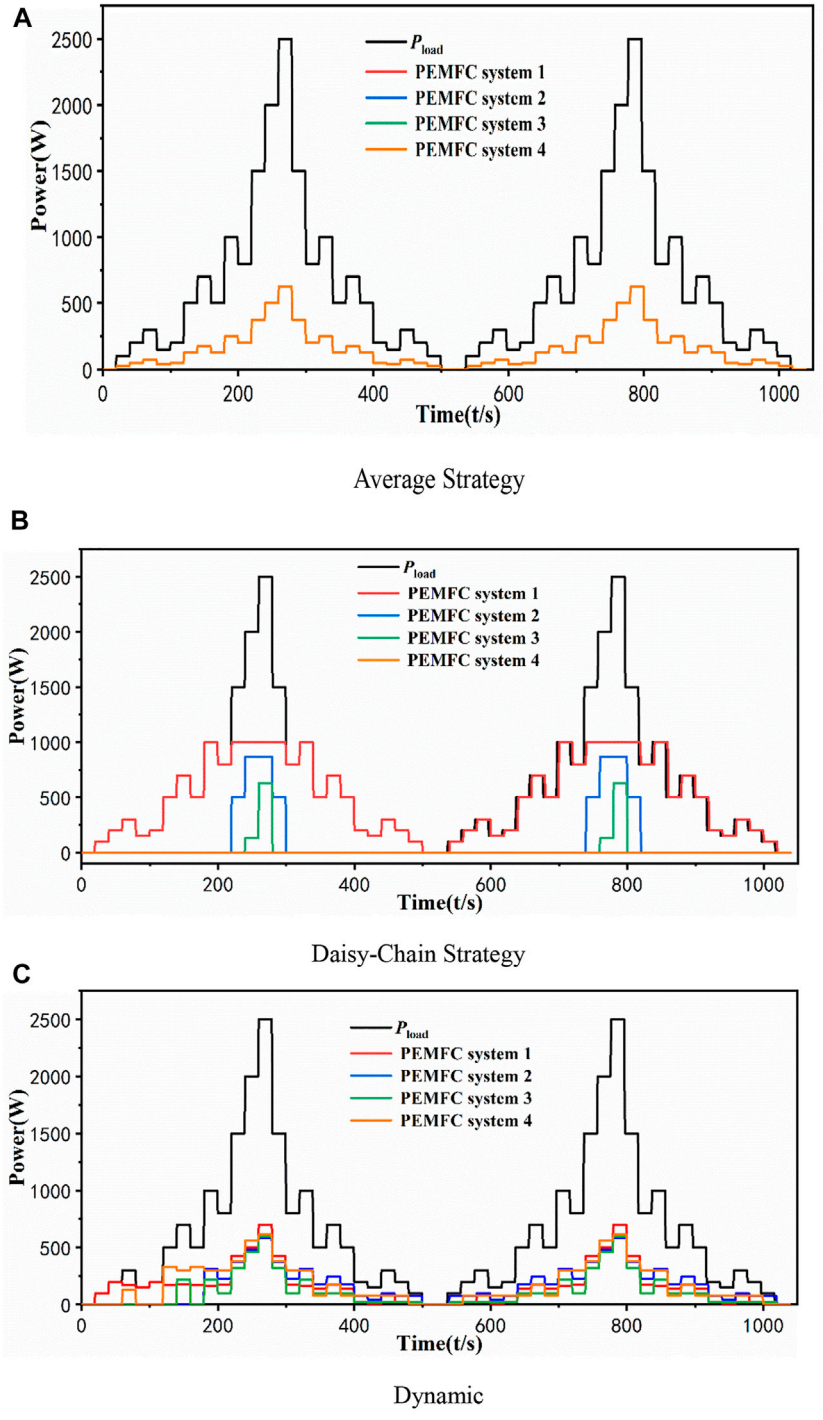

FIGURE 8
Power strategy Comparison. **(A)** Average strategy. **(B)** Daisy-chain strategy. **(C)** Dynamic.

consumption of the fan, controller, and other auxiliary components increases with increased P_{load}. Therefore, the corresponding system efficiency is also the lowest, as shown in Figure 9B.

The hydrogen consumption and efficiency of the MFC system with strategies are shown in Table 3. The discrete optimization strategy has the best performance, saving 2.35% in hydrogen consumption, increasing the average efficiency by

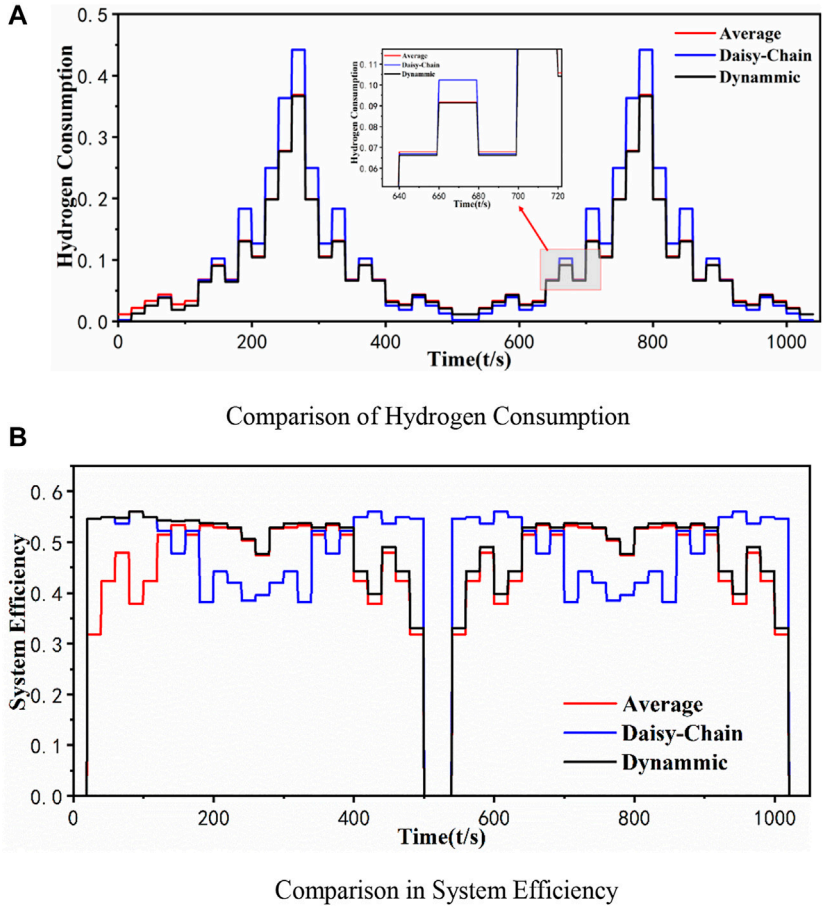

FIGURE 9
Comparison of different strategies. **(A)** Comparison of hydrogen consumption. **(B)** Comparison in system efficiency.

TABLE 3 Performance of different strategies.

Allocation strategy	Average fuel consumption (g)	Total fuel consumption (g)	Average efficiency (%)	Max efficiency (%)
Average	0.089053	92.61511	43.5641	53.3425
Daisy chain	0.10168	105.7473884	45.3626	55.9867
Dynamic Programming	0.086952	90.42983	45.881	55.9867

2.3169% compared to the average strategy, reducing 12.4% in hydrogen consumption, and increasing the average efficiency by 0.51% compared to the Daisy-chain strategy. The Daisy chain has the same maximum efficiency as the discrete seeking strategy because the system corresponding to that point activates one stack with operational efficiency, which shows that the discrete seeking strategy adopts advantages of the Daisy-chain method.

6.3 Stack failure response analysis

It is assumed that the controller disconnects the failed stack and switches the power allocation strategy from four-stack to three-stack when one stack fails. This is represented in Simulink as a switchover for lookup-table modules.

The strategy proposed has a positive performance effect on system failure. According to the approach in Yan et al., 2020,

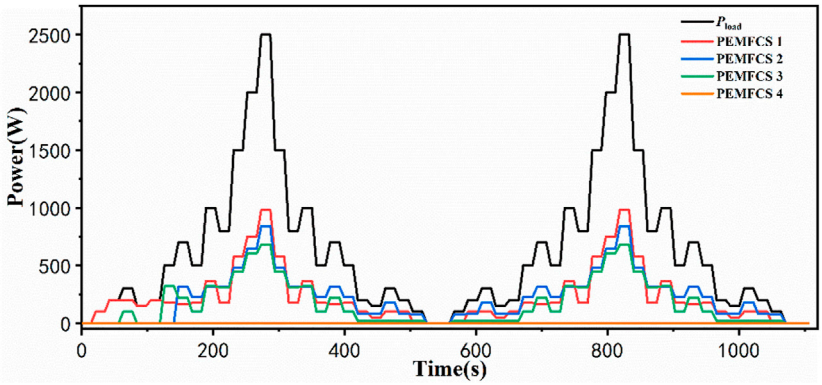

FIGURE 10
Stack No.4 with fails at the MFC system start.

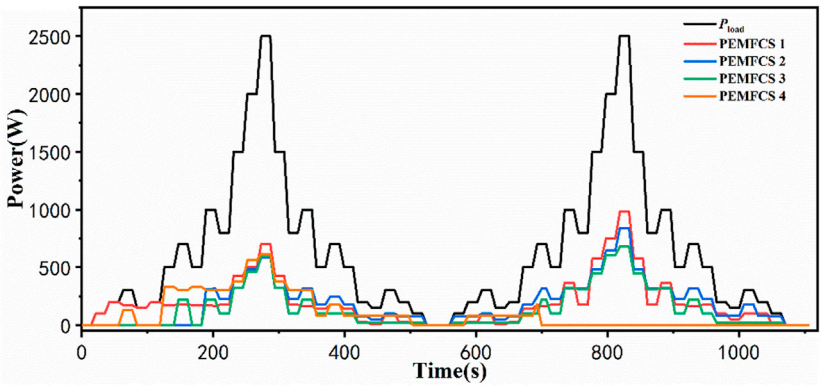

FIGURE 11
Stack No.4 with fails at the 200th second.

assumed No.4 stack failed. The outcome of power allocation is a failure of the No.4 stack at various times, as shown in Figures 9, 10. In case 1, stack No.4 fails at MFC system start and has no operation, so $C_{fcs4} = 0$ as shown in Figure 10. In case 2, stack No.4 fails at the 700th second, and subsystem 1–3's output power is higher in stages 2 and 3. It indicated that the No.4 stack is turned off on failure. The remaining subsystems increased the output power to satisfy load and ensure system stability after recalculating, as shown in Figure 11.

7 Conclusion

This study discretizes the load-hydrogen consumption curves of the single stack. It adopts the DP algorithm to obtain the power allocation strategy of MFCS with hydrogen consumption as the target in a backward derivation. It is found that the activated state of the single-stack system impacts the power allocation strategy because stacks do not respond to the load power when it starts up but still consume power when it has to maintain the controller and the fan operation, notably existing in water-cooled stacks. Therefore, two types of strategies are formed when the stack start-up state is considered in the study . Finally, the controller disconnects the failed fuel cell subsystem and then switches the power allocation strategy when one FC fails.

All the abovementioned operation processes are done in Simulink, and this MFC system is composed of four fuel cell subsystems, and the FC parameters are experimentally measured. The simulation results show that the power allocation strategy proposed in this paper has less hydrogen consumption than others, which is only 90.42983g, and the average efficiency is 45.881% and is the highest. The same maximum efficiency as the Daisy chain is available due to the avoidance of additional auxiliary losses by starting fewer fuel cell subsystems in the low power range.

However, this strategy cannot control MFCS online because FC decreases continuously with the operating time and frequent start-ups. This means that the FC's maximum power and load–hydrogen consumption curve constantly evolve. Nevertheless, the power allocation strategy with the DP algorithm provides a reference for other methods as an optimal power allocation strategy.

Data availability statement

The datasets presented in this article are not readily available because the data are provided by the cooperative manufacturer and they are not convenient to upload. Requests to access the datasets should be directed to YL, YFanliang@yeah.net.

Author contributions

YL: methodology, software, validation, formal analysis, and writing the original draft. QL: review and supervision. JZ: conceptualization, resources, and writing–review and editing. JH: software, validation, and visualization.

Conflict of interest

The authors declare that the research was conducted in the absence of any commercial or financial relationships that could be construed as a potential conflict of interest.

Publisher's note

All claims expressed in this article are solely those of the authors and do not necessarily represent those of their affiliated organizations or those of the publisher, the editors, and the reviewers. Any product that may be evaluated in this article or claim that may be made by its manufacturer is not guaranteed or endorsed by the publisher.

References

Abuzant, Sondos, Jemei, S., Hissel, D., Boulon, L., Agbossou, K., Gustin, F., et al. (2017). A review of multi-stack PEM fuel cell systems: Advantages, challenges and on-going applications in the industrial market. *IEEE Veh. Power Propuls. Conf. (VPPC)* 2017, 1–6. doi:10.1109/VPPC.2017.8330971

Andújar, J. M., Vivas, F. J., Segura, F., and Calderon, A. (2022). Integration of air-cooled multi-stack polymer electrolyte fuel cell systems into renewable microgrids. *Int. J. Electr. Power & Energy Syst.* 142, 108305. doi:10.1016/j.ijepes.2022.108305

Becherif, Mohamed, Claude, F., Hervier, T., and Boulon, L. (2015). Multi-stack fuel cells powering a vehicle. *Energy procedia*. 74, 308–319. doi:10.1016/j.egypro.2015.07.613

Bouisalmane, Noureddine, Gao, Fei, Levy, Michael, Paire, Damien, Doubabi, Saïd, Breaz, Elena, et al. (2021). Hydrogen consumption minimization with optimal power allocation of multi-stack fuel cell system using particle swarm optimization. *IEEE Transp. Electrification Conf. Expo (ITEC)* 2021, 154–160. doi:10.1109/ITEC51675.2021.9490111

Calderón, A. J., Vivas, F. J., Segura, F., and Andujar, J. M. (2020). Integration of a multi-stack fuel cell system in microgrids: A solution based on model predictive control. *Energies* 13 (18), 4924. doi:10.3390/en13184924

Cardozo, John (2015). "Comparison of multi-stack fuel cell system architectures for residential power generation applications including electrical vehicle charging," in IEEE Vehicle Power and Propulsion Conference (VPPC), Montreal, QC, Canada, 19-22 October 2015 (IEEE).2015

Cheng, G., Hao, L., Chen, X., and Shaoming, Q. (2015). "Parameter design of the powertrain of fuel cell electric vehicle and the energy management strategy," in 34th Chinese Control Conference (CCC), Hangzhou, China, 28-30 July 2015 (IEEE), 8027–8032.2015

De Bernardinis, A., Marion-Péra, M.-C., Garnier, J., and Hissel, D. (2008). Fuel cells multi-stack power architectures and experimental validation of 1 kW parallel twin stack PEFC generator based on high frequency magnetic coupling dedicated to on board power unit. *Energy Convers. Manag.* 49 (8), 2367–2383. doi:10.1016/j.enconman.2008.01.022

Fernandez, Alvaro Macias, Kandidayeni, M., Boulon, L., and Chaoui, H. (2019). An adaptive state machine based energy management strategy for a multi-stack fuel cell hybrid electric vehicle. *IEEE Trans. Veh. Technol.* 69 (1), 220–234. doi:10.1109/tvt.2019.2950558

Garcia, Jorge E., Sicard, P., Boulon, L., Vega, D. H., et al. (2014). Power sharing for efficiency optimisation into a multi fuel cell system. *IEEE 23rd Int. Symposium Industrial Electron. (ISIE)* 2014, 218–223. doi:10.1109/ISIE.2014.6864614

Han, Xu, Li, F., Zhang, T., Zhang, T., and Song, K. (2017). Economic energy management strategy design and simulation for a dual-stack fuel cell electric vehicle. *Int. J. Hydrogen Energy* 42 (16), 11584–11595. doi:10.1016/j.ijhydene.2017.01.085

Jian, B., and Wang, H. (2022). Hardware-in-the-loop real-time validation of fuel cell electric vehicle power system based on multi-stack fuel cell construction. *J. Clean. Prod.* 331, 129807. doi:10.1016/j.jclepro.2021.129807

Kristianda, Febrian (2018). Estimation of vector autoregressive model's parameter using genetic algorithm. *Int. Symposium Adv. Intelligent Inf. (SAIN)* 2018, 72–77. doi:10.1109/SAIN.2018.8673382

Li, X., Shang, Z., Peng, F., Li, L., Zhao, Y., and Liu, Z. (2021). Increment-oriented online power distribution strategy for multi-stack proton exchange membrane fuel cell systems aimed at collaborative performance enhancement. *J. Power Sources* 512, 230512. doi:10.1016/j.jpowsour.2021.230512

Liu, Jichao, Chen, Y., Li, W., Shang, F., and Zhan, J. (2017). Hybrid-trip-model-based energy management of a PHEV with computation-optimized dynamic programming. *IEEE Trans. Veh. Technol.* 67 (1), 338–353. doi:10.1109/tvt.2017.2777852

Lopes, Da Costa, Boulon, Loic, Kelouwani, S., Agbossou, K., Marx, Neigel, Ettihir, Khalid, et al. (2016). Neural network modeling strategy applied to a multi-stack PEM fuel cell system. *IEEE Transp. Electrification Conf. Expo (ITEC)* 2016, 1–7. doi:10.1109/ITEC.2016.7520294

Macias, A., Kandidayeni, M., Boulon, L., and Chaoui, H. (2018). "A novel online energy management strategy for multi fuel cell systems," in IEEE International Conference on Industrial Technology (ICIT), Lyon, France, 20-22 February 2018 (IEEE).2018

Marx, N., Cárdenas, D. C. T., Boulon, L., Gustin, F., and Hissel, D. (2014). "Degraded mode operation of multi-stack fuel cell systems," in IEEE Vehicle Power and Propulsion Conference (VPPC), Coimbra, Portugal, 27-30 October 2014 (IEEE), 1–6. doi:10.1109/VPPC.2014.70070412014

Marx, Neigel, Boulon, L., Gustin, F., Hissel, D., and Agbossou, K. (2014). A review of multi-stack and modular fuel cell systems: Interests, application areas and on-going research activities. *Int. J. Hydrogen Energy* 39 (23), 12101–12111. doi:10.1016/j.ijhydene.2014.05.187

Marx, N., Hissel, D., Gustin, F., Boulon, L., and Agbossou, K. (2017). On the sizing and energy management of an hybrid multistack fuel cell – battery system for automotive applications[J]. *Int. J. Hydrogen Energy* 42, 1518–1526. doi:10.1016/j.ijhydene.2016.06.111

Marx, N., Hissel, D., Gustin, F., and Boulon, L. (2018). "On maximizing the steady-state efficiency of a multi-stack fuel cell system," in IEEE Vehicle Power and Propulsion Conference (VPPC), Chicago, IL, USA, 27-30 August 2018 (IEEE), 1–6. doi:10.1109/VPPC.2018.8605036

Meng, Xiang, Li, Q., Huang, T., Wang, X., Zhang, G., and Chen, W. (2020). A distributed performance consensus control strategy of multistack PEMFC generation system for hydrogen EMU trains. *IEEE Trans. Ind. Electron.* 68 (9), 8207–8218. doi:10.1109/tie.2020.3016243

Musio, Fabio, Tacchi, F., Omati, L., Gallo Stampino, P., Dotelli, G., Limonta, S., et al. (2011). PEMFC system simulation in MATLAB-Simulink® environment. *Int. J. Hydrogen Energy* 36 (13), 8045–8052. doi:10.1016/j.ijhydene.2011.01.093

Musio, Fabio, Tacchi, F., Omati, L., Gallo Stampino, P., Dotelli, G., Limonta, S., et al. (2011). PEMFC system simulation in MATLAB-Simulink® environment. *Int. J. Hydrogen Energy* 36 (13), 8045–8052. doi:10.1016/j.ijhydene.2011.01.093

Pirasaci, Tolga (2019). Non-uniform, multi-stack solid oxide fuel cell (SOFC) system design for small system size and high efficiency. *J. Power Sources* 426, 135–142. doi:10.1016/j.jpowsour.2019.04.037

Salim, Reem, Nabag, M., Noura, H., and Fardoun, A. (2015). The parameter identification of the Nexa 1.2 kW PEMFC's model using particle swarm optimization. *Renew. Energy* 82, 26–34. doi:10.1016/j.renene.2014.10.012

Wang, T., Li, Q., Yin, L., and Chen, W. (2019). Hydrogen consumption minimization method based on the online identification for multi-stack PEMFCs system. *Int. J. hydrogen energy* 44 (11), 5074–5081. doi:10.1016/j.ijhydene.2018.09.181

Wang, Tianhong, Li, Q., Wang, X., Chen, W., Breaz, E., and Gao, F. (2020). A power allocation method for multistack PEMFC system considering fuel cell performance consistency. *IEEE Trans. Ind. Appl.* 56 (5), 5340–5351. doi:10.1109/tia.2020.3001254

Wang, Tianhong, Li, Q., Yang, H., Yin, L., Wang, X., Qiu, Y., et al. (2019). Adaptive current distribution method for parallel-connected PEMFC generation system considering performance consistency. *Energy Convers. Manag.* 196, 866–877. doi:10.1016/j.enconman.2019.06.048

Yan, Yu, Li, Q., Chen, W., Huang, W., Liu, J., and Liu, J. (2020). Online control and power coordination method for multistack fuel cells system based on optimal power allocation. *IEEE Trans. Ind. Electron.* 68 (9), 8158–8168. doi:10.1109/tie.2020.3016240

Zhang, Caizhi, Zeng, T., Wu, Q., Deng, C., Chan, S. H., and Liu, Z. (2021). Improved efficiency maximization strategy for vehicular dual-stack fuel cell system considering load state of sub-stacks through predictive soft-loading. *Renew. Energy* 179, 929–944. doi:10.1016/j.renene.2021.07.090

Zhang, Shuo, and Xiong, Rui (2015). Adaptive energy management of a plug-in hybrid electric vehicle based on driving pattern recognition and dynamic programming. *Appl. Energy* 155, 68–78. doi:10.1016/j.apenergy.2015.06.003

Zhou, S., Zhang, G., Fan, L., Gao, J., and Pei, F. (2022). Scenario-oriented stacks allocation optimization for multi-stack fuel cell systems. *Appl. Energy* 308, 118328. doi:10.1016/j.apenergy.2021.118328

Zhou, Su, Zhang, G., Fan, L., Gao, J., and Pei, F. (2022). Scenario-oriented stacks allocation optimization for multi-stack fuel cell systems. *Appl. Energy* 308, 118328. doi:10.1016/j.apenergy.2021.118328